IJEMD-M, 3 (1) (2025) https://doi.org/10.54938/ijemdm.2025.03.1.563

International Journal of Emerging Multidisciplinaries: Mathematics

Research Paper

Journal Homepage: www.ojs.ijemd.com
ISSN (print): 2790-1998

Exploration of Arrhenius Activation Energy on Hybrid Nanofluid Over a Rotating Radially Stretching Disk

Mahnoor Maqsood [1], Azeem Shahzad [1], Tahir Naseem [2,3] *, Shoaib Ali [1]

1. Department of Mathematical Sciences, University of Engineering and Technology, Taxila, 47050, Pakistan

2. Pak-Austria Fach Hochschule: Institute of Applied Sciences and Technology (PAF-IAST), 22600, Pakistan

3. Government Degree College Khanpur, Haripur, 22620, Pakistan

Abstract

In this study, the Arrhenius energy of activation and viscous dissipation on the magnetohydrodynamic (MHD) flow of a hybrid nanofluid, namely, ($Cu - Al_2O_3$/water), in a rotating radially stretching disk are examined. Similarity variables are then used to reduce the governing partial differential equations (PDEs) of momentum, energy, and concentration to a system of coupled ordinary differential equations (ODEs). The resulting nonlinear boundary value problem is numerically solved in MATLAB using the bvp5c solver. The effect of major physical parameters of the Hartmann number (Ha), Eckert number (Ec), Prandtl number (Pr), the Schmidt number (Sc), and the activation energy parameter on the velocity, temperature, and concentration profiles are discussed. Hartmann number (Ha) kills velocity profiles, however, it promotes temperature distribution. The Eckert number (Ec) significantly increases thermal boundary layer thickness due to viscous heating, while activation energy (E) strengthens mass transfer. Furthermore, the hybrid nanofluid ($Cu - Al_2O_3$/water) shows superior thermal performance compared to unitary nanofluids. A key finding is that the interplay between the magnetic field (Ha) and activation energy (E) creates a competing mechanism, where Ha suppresses mass diffusion while E enhances it, with significant implications for reactive flow control. This work offers insights into optimizing thermal systems that involve rotating disks, such as turbomachinery and renewable energy applications.($Cu - Al_2O_3$/water).

Keywords: Hybrid Nanofluid; Arrhenius Activation Energy; Rotating and Stretching Disk; Viscous Dissipation; Magnetohydrodynamic (MHD).

Email Address: tahir.naseem@paf-iast.edu.pk (Tahir Naseem *)

Nomenclature

Nomenclature			
(r, θ, z)	Cylindrical coordinates	B_0	Magnetic Strength
α	Thermal Diffusivity	L_1	Velocity slip factor
(u, v, w)	Velocity Component	L_2	Thermal slip factor
Nu	Nusselt Number	L_3	Concentration slip factor
Pr	Prandtl Number	T_∞	Ambient Temperature (K)
Sc	Schmidt Number	C_∞	Ambient Concentration $(molm^{-3})$
Ha	Hartmann number	C	Fluid's Concentration $(molm^{-3})$
C_p	Specific Heat at constant$(JK^{-1}kg^{-1})$	D_B	Brownian motion factor, (m^2s^{-2})
ρ_{hnf}	Density of Hybrid Nanofluid (kgm^{-3})	E_a	Activation energy, $(kg.m^2s^{-2})$
ν	Kinematic viscosity	k_r	Chemical reaction rate constant $(molm^{-3}s^{-1})$
T	Temperature of the fluid (K)	Ec	Eckert number
μ	Viscosity	η	Dimensionless variable
Ω	Angular velocity	λ	Stretching rate
Q	heat source/sink		

1. Introduction

Hybrid nanofluids, formed as a result of adding two or more nanoparticles of different types to a base fluid, are a novel potential class of working fluids in thermal engineering applications. Hybrid nanofluids have excellent thermophysical properties like high thermal conductivity, improved suspension stability, and regulated viscosity as compared to conventional fluids and even simple nanofluids, making them very effective in cooling and energy systems.

Arrhenius activation energy is another significant concept in transport phenomena, and it is the minimum energy needed in order to have a chemical reaction take place. In reactive flows, activation energy is an important factor in the distribution of the concentration through either decelerating the mass transfer processes or accelerating them. It is especially significant when the hybrid nanofluids are examined under chemical active conditions.

The concept of nanofluids was first introduced in the mid-1990s, where the suspension of nanoparticles in conventional base fluids was shown to significantly enhance thermal conductivity [1]. Since then, extensive research has been carried out on nanofluids for various applications including cooling systems, energy devices, and electronic equipment. However, to achieve even greater performance, the idea of hybrid nanofluids was later developed, where two or more types of nanoparticles are dispersed into a base fluid to combine their synergistic properties [2], [3].

[4] conducted one of the earliest experimental investigations on $Cu - Al_2O_3$/water hybrid nanofluids and observed a 30% improvement in thermal conductivity compared to conventional nanofluids. Nine et al. [5] further emphasized the importance of nanoparticle shape and combination, reporting enhanced thermal properties while maintaining stable viscosity behavior. Similarly, [6] and [7] demonstrated that graphene oxide-based hybrid nanofluids provide excellent thermal performance due to the high intrinsic conductivity of graphene when combined with metallic nanoparticles.

In addition to the advancement of hybrid nanofluids, studies have considered several physical effects influencing transport phenomena. For instance, the role of activation energy in chemically reactive flows was analyzed by [8], who highlighted its importance in modifying diffusion and reaction rates. Rotating and stretching disk problems have also attracted considerable attention since Von Kármán's pioneering work [9], with applications in turbine cooling, rotating machinery, and polymer processing. [10] provided analytical solutions for boundary layer flow over stretching surfaces, establishing their industrial relevance. Stretching surfaces with different geometries and boundary conditions are investigated by various scholar [12-16].

Viscous dissipation has been another significant factor in hybrid nanofluid analysis. [17] studied the influence of viscous dissipation and non-uniform heating, showing that it plays a vital role in modifying the thermal boundary layer. Magnetohydrodynamic (MHD) effects have also been extensively investigated in nanofluid systems due to their applications in electrically conducting flows. [18] presented exact solutions for MHD flow in rotating disk systems, demonstrating the strong effect of the magnetic parameter (Hartmann number) on velocity and temperature distributions.

To solve the highly nonlinear equations arising in hybrid nanofluid problems, numerical methods are often employed. [19] introduced the MATLAB bvp5c solver, which has since been widely applied to boundary value problems involving complex nonlinear systems. This approach ensures high accuracy and stability, making it particularly suitable for hybrid nanofluid flow analysis.

Recently, $Cu - Al_2O_3$/water hybrid nanofluids have been studied extensively due to their excellent balance of thermal conductivity and stability. [6] and [20] confirmed that the combination of copper and alumina nanoparticles in water provides enhanced heat transfer capabilities compared to mono-

particle nanofluids. Their unique thermophysical properties make them an attractive choice for modern industrial and thermal applications.

Building upon these developments, the present study focuses on the three-dimensional flow of $Cu - Al_2O_3$/water hybrid nanofluid over a rotating radially stretching disk, incorporating viscous dissipation, magnetohydrodynamic effects, and Arrhenius activation energy. While recent studies like [21] and [27] have analyzed activation energy or rotating disks for nanofluids, the combined investigation of Arrhenius activation energy, viscous dissipation, and three slip conditions (velocity, thermal, concentration) for a $Cu - Al_2O_3$/water hybrid nanofluid over a radially stretching and rotating disk remains unexplored. This study aims to fill this gap. The governing equations are solved using the bvp5c numerical method, and the influence of key parameters such as the Hartmann number, Eckert number, Prandtl number, Schmidt number, and activation energy on velocity, temperature, and concentration fields is systematically investigated.

2. Mathematical Formulation

we consider the three-dimensional flow of a $Cu - Al_2O_3$/water hybrid nanofluid over a rotating radially stretching disk using cylindrical coordinates (r, θ, z). The disk stretches radially outward in the $r -$ direction while simultaneously rotating with angular velocity in the $\theta -$ direction, creating a complex boundary layer flow. A uniform magnetic field B_0 is applied normal to the disk surface (along the $z -$ axis), which introduces magnetohydrodynamic (MHD) effects on the electrically conducting hybrid nanofluid. Additionally, viscous dissipation is taken into account, representing the conversion of kinetic energy into thermal energy due to internal fluid friction. The concentration equation incorporates the effect of Arrhenius activation energy, which influences mass transfer in reactive flows.

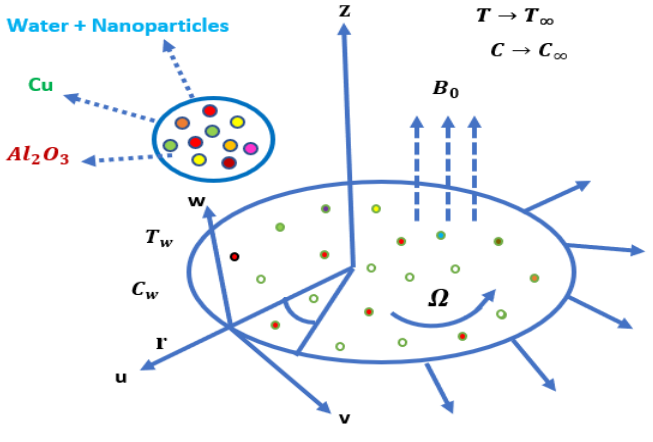

Fig. 1. Model representation of Physical Phenomena

The real-world phenomenal model depicted mathematically is illustrated in (Fig. 1.) by cylindrical co-ordinates (r, θ, z).

Accordingly, from the basic governing equation for momentum, energy and concentration the following as [15].

$$\frac{\partial u}{\partial r}+\frac{u}{r}+\frac{\partial w}{\partial z}=0, \tag{1}$$

$$\rho_{hnf}\left(u\frac{\partial u}{\partial r}+w\frac{\partial u}{\partial z}\right)=\mu_{hnf}\left[\frac{\partial^2 u}{\partial r^2}+\frac{1}{r}\frac{\partial u}{\partial r}-\frac{u}{r^2}+\frac{\partial^2 u}{\partial z^2}\right]+\frac{v^2}{r}-\sigma_{hnf}B_0^2 u \tag{2}$$

$$\rho_{hnf}\left(u\frac{\partial v}{\partial r}+w\frac{\partial v}{\partial z}\right)=\mu_{hnf}\left[\frac{\partial^2 v}{\partial r^2}+\frac{1}{r}\frac{\partial v}{\partial r}-\frac{v}{r^2}+\frac{\partial^2 v}{\partial z^2}\right]-\frac{uv}{r}-\sigma_{hnf}B_0^2 v, \tag{3}$$

$$\rho_{hnf}\left(u\frac{\partial w}{\partial r}+w\frac{\partial w}{\partial z}\right)=\mu_{hnf}\left[\frac{\partial^2 w}{\partial r^2}+\frac{1}{r}\frac{\partial w}{\partial r}+\frac{\partial^2 w}{\partial z^2}\right]-\frac{\partial p}{\partial z}, \tag{4}$$

$$u\frac{\partial T}{\partial r}+w\frac{\partial T}{\partial z}=\frac{k_{hnf}}{(\rho C_p)_{hnf}}\left[\frac{\partial^2 T}{\partial r^2}+\frac{1}{r}\frac{\partial T}{\partial r}+\frac{\partial^2 T}{\partial z^2}\right]+\frac{\mu_{hnf}}{\left(\rho C_p\right)_{hnf}}\left(\frac{\partial u}{\partial r}\right)^2+\frac{Q}{\left(pC_p\right)_{hnf}}(T-T_\infty), \tag{5}$$

$$u\frac{\partial C}{\partial r}+w\frac{\partial C}{\partial z}=D_B\left[\frac{\partial^2 C}{\partial r^2}+\frac{1}{r}\frac{\partial C}{\partial r}+\frac{\partial^2 C}{\partial z^2}\right]-K_r^2(C-C_\infty)\left(\frac{T}{T_\infty}\right)^n exp\left(-\frac{E_a}{\kappa T}\right), \tag{6}$$

Boundary conditions are:

$$u=\lambda+L_1\frac{\partial u}{\partial z}, \tag{7}$$

$$v=r\Omega+L_1\frac{\partial v}{\partial z},\quad w=0,\quad T=T_w+L_2\frac{\partial T}{\partial z},\quad C=C_w+L_3\frac{\partial C}{\partial z}\ at\ z=0$$

$$u\to 0,\qquad v\to 0,\qquad T\to T_\infty,\qquad C\to C_\infty\ at\quad z\to\infty \tag{8}$$

Where $u, v\ and\ w$ are velocity along $x, y\ and\ z-$ axis respectively. Where L_1 is the slip factor of velocity, L_2 is the thermal concentration, L_3 is the concentration slip factor, μ_{hnf} is the dynamic viscosity coefficient, ρ_{hnf} is the effective density of the hybrid nanofluid, B_0 is the applied magnetic field, C_p is specific heat of fluid, $(\rho C_p)_{hnf}$ is the effective heat capacity of the hybrid nanofluid, σ_{hnf} is the electrical conductivity of the liquid, T is temperature of the fluid, and T_∞ is the ambient temperature of fluid and rate of reaction is represented by k_r , C denotes the concentration, C_∞ represents the ambient concentration, D_B is the Brownian factor, E_a is the energy used to activate, and κ is the Boltzmann constant [23].

The definition of thermal and physical parameters of the hybrid nanofluid are as follows [18].

The dynamic viscosity of hybrid nanofluid μ_{hnf} takes the form of.

$$\mu_{hnf}=\frac{\mu_f}{(1-\varphi_1)^{2.5}(1-\varphi_2)^{2.5}} \tag{9}$$

The heat capacity of hybrid nanofluid $(\rho C_p)_{hnf}$ and density of hybrid nanofluid ρ_{hnf} are presented as follows:

$$\rho_{hnf} = \rho_f \left(\varphi_1 \frac{\rho_{s1}}{\rho_f} + 1 - \varphi_1 \right)(1 - \varphi_2) + \rho_{s2}\varphi_2 \tag{10}$$

$$(\rho C_p)_{hnf} = (\rho C_p)_f (1 - \varphi_2) \left(\varphi_1 \frac{(\rho C_p)_{s1}}{(\rho C_p)_f} + (1 - \varphi_1) \right) + \varphi_2 (\rho C_p)_{s2} \tag{11}$$

In this case Maxwell-Garnet model [19] is included in the form of conductivity k_{hnf} as:

$$\left.\begin{aligned} \frac{k_{hnf}}{k_{nf}} &= \frac{k_{s2} - 2\varphi_2(k_{nf} - k_{s2}) + 2k_{nf}}{k_{s2} + \varphi_2(k_{nf} - k_{s2}) + 2k_{nf}}, \\ \frac{k_{nf}}{k_f} &= \frac{k_{s1} - 2\varphi_1(k_f - k_{s1}) + 2k_f}{k_{s1} + \varphi_1(k_{nf} - k_{s2}) + 2k_f} \end{aligned}\right\} \tag{12}$$

Moreover, the electrical conductivity σ_{hnf} of the hybrid nanofluid.

$$\frac{\sigma_{hnf}}{\sigma_f} = 1 + \frac{3\left(\frac{\sigma_1\varphi_1 + \sigma_2\varphi_2}{\sigma_f} - (\varphi_1 + \varphi_2) \right)}{2 + \left(\frac{\sigma_1\varphi_1 + \sigma_2\varphi_2}{\sigma_f(\varphi_1 + \varphi_2)} \right) - \left(\left(\frac{\sigma_1\varphi_1 + \sigma_2\varphi_2}{\sigma_f} \right) - (\varphi_1 + \varphi_2) \right)} \tag{13}$$

φ_1 and φ_2 are the volume fractions of the nano size particles Cu and Al_2O_3 and the subscripts represent the base as f, nano-fluid is represented by the subscripts and hybrid nano-fluid levels are represented by the subscripts used in the Eqs. (10) – (13). Table 1 gives the relations of the alumina, cupper and water.

By using the similarity transformations [26] as below:

$$\left.\begin{aligned} u = r\Omega f'(\eta), \qquad v = r\Omega g(\eta), \qquad w = -\sqrt{2\Omega\mathcal{V}_f} f(\eta) \\ \eta = z\sqrt{\frac{2\Omega}{\mathcal{V}_f}}, \quad \theta(\eta) = \frac{T - T_\infty}{T_w - T_\infty}, \qquad \phi(\eta) = \frac{C - C_\infty}{C_w - C_\infty} \end{aligned}\right\} \tag{14}$$

The set of similarity transformations discussed complied with this law of conservation of mass as depicted in the equation (1). Therefore, the analytical problem set out by the Eqs. (2) – (8) is changed with a set of ordinary differential equations as follows:

$$2\frac{A_1}{A_2} f''' + 2ff'' - f'^2 + g^2 - \frac{A_3}{A_2}(Ha)^2 f' = 0 \tag{15}$$

$$2\frac{A_1}{A_2} g'' + 2fg' - 2f'g - \frac{A_3}{A_2}(Ha)^2 g = 0 \tag{16}$$

$$\frac{1}{Pr}\frac{A_4}{A_5}\theta'' + f\theta' + \delta_1\theta + \frac{A_1}{A_5} \in_1 E_c f''^2 = 0 \tag{17}$$

$$\frac{2}{S_c}\phi'' + 2f\phi' + \sigma(1+\delta\theta)^n\phi\exp\left(\frac{-E}{1+\delta\theta}\right) = 0 \tag{18}$$

$$\left.\begin{array}{c} f(0)=0,\ f'(0)=\lambda+\alpha f''(0),\quad g(0)=1+\alpha g'(0), \\ \theta(0)=1+\beta\theta'(0),\ \ \phi(0)=1+\gamma\phi'(0), \\ f'(\infty)\to 0,\qquad g(\infty)\to 0,\qquad \theta(\infty)\to 0,\qquad \phi(\infty)\to 0 \end{array}\right\}, \tag{19}$$

Where

$$A_1 = (1-\varphi_1)^{2.5}(1-\varphi_2)^{2.5},$$

$$A_2 = \rho_f\left(\varphi_1\frac{\rho_{s1}}{\rho_f} + 1 - \varphi_1\right)(1-\varphi_2) + \rho_{s2}\varphi_2,$$

$$A_3 = 1 + \frac{3\left(\frac{\sigma_1\varphi_1+\sigma_2\varphi_2}{\sigma_f} - (\varphi_1+\varphi_2)\right)}{2 + \left(\frac{\sigma_1\varphi_1+\sigma_2\varphi_2}{\sigma_f(\varphi_1+\varphi_2)}\right) - \left(\left(\frac{\sigma_1\varphi_1+\sigma_2\varphi_2}{\sigma_f}\right) - (\varphi_1+\varphi_2)\right)},$$

$$A_4 = \frac{k_{s2} - 2\varphi_2\left(k_{nf}-k_{s2}\right) + 2k_{nf}}{k_{s2} + \varphi_2\left(k_{nf}-k_{s2}\right) + 2k_{nf}},$$

$$A_5 = (\rho C_p)_f(1-\varphi_2)\left(\varphi_1\frac{\left(\rho C_p\right)_{s1}}{\left(\rho C_p\right)_f} + (1-\varphi_1)\right) + \varphi_2\left(\rho C_p\right)_{s2}.$$

Where $\alpha = L_1\sqrt{\frac{2\Omega}{\nu}}$ is used for the velocity slip parameter, $\beta = L_2\sqrt{\frac{2\Omega}{\nu}}$ represents thermal slip parameter, $\gamma = L_3\sqrt{\frac{2\Omega}{\nu}}$ shows the concentration slip parameter, λ is the stretching parameter, $Pr = \frac{\nu}{\alpha_{hnf}}$ indicated as Prandtl number, $(Ha)^2 = \frac{\sigma B_0^2}{\Omega\rho_{hnf}}$ is the Hartmann number, $S_c = \frac{\nu}{D_B}$ is the Schmidt number, $Ec = \frac{U^2}{C_p(T_w - T_\infty)}$ is the Eckert number, $\sigma = \frac{K_r^2}{\Omega}$ for reaction parameters, $\delta_1 = \frac{Q}{2\Omega(\rho C_p)_{hnf}}$ is used for the parameter of heat absorption/generation, $\delta = \frac{T_w - T_\infty}{T_\infty}$ is for temperature difference, $E = \frac{E_a}{kT_\infty}$ is used for nondirectional activation energy, $\alpha_{hnf} = \frac{k}{(\rho C_p)_{hnf}}$ is the thermal diffusivity. Table 1 presents the physical properties of the nanoparticles and base fluid.

Table 1. Thermophysical characteristics of water, alumina, and copper [27]:

Physical Properties	H_2O (water)	Al_2O_3 (alumina)	Cu (copper)
ρ (kg/m³)	997.1	3970	8933
Cp (J·kg⁻¹·K⁻¹)	4179	765	385
k (W·m⁻¹·K⁻¹)	0.6132	40	401
σ (Ω·m)⁻¹	5.5×10^{-6}	1×10^{-12}	5.96×10^{7}

The practical interest quantities are the coefficient of skin friction C_f and the local Nusselt number Nu that can be defined as:

$$C_{fx} = \frac{\tau_{wx}}{\rho_{hnf} v_{1w}^2}, \qquad C_{fy} = \frac{\tau_{wy}}{\rho_{hnf} v_{1w}^2}, \qquad Nu_x = \frac{x q_w}{k_{nf}(T_s - T_\infty)} \tag{20}$$

The terms $\tau_{wx} = \tau_{zx}|_{z=0}$, $\tau_{wy} = \tau_{zy}|_{z=0}$, q_w give rise to the following relations as:

$$\tau_{wx} = \mu_{hnf} \left.\frac{\partial v_1}{\partial z}\right|_{z=0}, \qquad \tau_{wy} = \mu_{hnf} \left.\frac{\partial v_2}{\partial z}\right|_{z=0}, \qquad q_w = q_r|_{z=0} - k_{hnf} \left.\frac{\partial T}{\partial z}\right|_{z=0} \tag{21}$$

Substituting values, we get

$$\sqrt{Re_x} C_{fx} = f''(0) \frac{1}{(1-\varphi_1)^{2.5}(1-\varphi_2)^{2.5}},$$

$$\sqrt{Re_x} C_{fy} = g'(0) \frac{1}{(1-\varphi_1)^{2.5}(1-\varphi_2)^{2.5}},$$

$$\frac{Sh_x}{\sqrt{Re_x}} = -\varphi'(0),$$

$$\frac{Nu_x}{\sqrt{Re_x}} = -\theta'(0)\left(\frac{k_{hnf}}{k_{nf}} + Rd\theta_w^3\right).$$

Here $Re_x = 2(\Omega x)x/v$ is the local Reynold number.

3. Numerical Approach

The non-linear terms in the segment's final regulating equations (2) – (6) make it challenging to find an analytical solution. The 3D flow of $Cu - Al_2O_3$/water hybrid nanofluid over a rotating radially stretching disk, incorporating MHD, viscous dissipation, and Arrhenius activation energy, are transformed into a system of dimensionless ODEs using similarity transformations. These equations are solved numerically in MATLAB using the bvp5c solver, which employs a collocation method to effectively handle boundary conditions. The accuracy of the results is ensured through the use of proper initial guesses, mesh refinement, and validation against limiting cases.

For use with a boundary-value solver, the system is written in first-order form by introducing

$$f = \zeta_1, f' = \zeta_2, f'' = \zeta_3, f''' = \zeta\zeta_1\,, g = \zeta_4\,, g' = \zeta_5,\ g'' = \zeta\zeta_2 \tag{22}$$
$$\theta = \zeta_6, \theta' = \zeta_7,\ \theta'' = \zeta\zeta_3$$
$$\varphi = \zeta_8, \varphi' = \zeta_9, \varphi'' = \zeta\zeta_4$$

$$\zeta\zeta_1 = \frac{A_2}{2A_1}\left(-2\zeta_1\zeta_3 - (\zeta_4)^2 + (\zeta_2)^2 + \frac{A_3}{A_2}(Ha)^2\zeta_2\right) \tag{23}$$

$$\zeta\zeta_2 = \frac{A_2}{2A_1}\left(2\zeta_2\zeta_4 - 2\zeta_1\zeta_5 + \frac{A_3}{A_2}(Ha)^2\zeta_4\right) \tag{24}$$

$$\zeta\zeta_3 = P_r\frac{A_5}{A_4}\left(-\zeta_1\zeta_7 - \frac{\delta_1}{2}\zeta_6 - \frac{A_1}{A_5}\in_1 E_c(\zeta_3)^2\right) \tag{25}$$

$$\zeta\zeta_4 = \frac{S_c}{2}\left(-2\zeta_1\zeta_9 - \sigma(1+\delta\zeta_6)^n\zeta_8 \exp\left(\frac{-E}{1+\delta\zeta_6}\right)\right) \tag{26}$$

The corresponding BC's are:

$$\left.\begin{array}{c}\zeta_0(1)=0,\quad \zeta_0(2)=\lambda+\alpha\zeta_0(3),\quad \zeta_0(4)=1+\alpha\zeta_0(5),\\ \zeta_0(6)=1+\beta\zeta_0(7),\quad \zeta_0(8)=1+\gamma\zeta_0(9)\end{array}\right\} \tag{27}$$

$$\zeta_\infty(2)\to 0,\qquad \zeta_\infty(4)\to 0,\qquad \zeta_\infty(6)\to 0,\qquad \zeta_\infty(8)\to 0 \tag{28}$$

Table 2. Comparison of the present and the existing results ($\boldsymbol{\varphi=0, \mathrm{Pr}=6.2}$).

Factors	Abd-Elmonem	Present
(f''(0))	0.51012517	0.51132469
(-g'(0))	0.60883001	0.62581123
(-θ'(0))	0.93276194	0.93167531

Table 2 expresses the comparative results of the present and the existing results. This assessment validates the numerical procedure.

4. Result and Discussion:

In this section, the impact of different physical parameters on the flow, temperature and concentration profiles of a hybrid nanofluid (Cu–Al_2O_3/water) over a rotating radially stretching disk is presented and discussed. The bvp5c solver of MATLAB was used to obtain the results.

Fig. 2 provides the variation in velocity profile with the increase in Hartmann number (Ha). It is found that at an increase in Ha the velocity of the nanofluid also decreases. The reason behind this is due to the fact that when the magnetic field is stronger, it produces a Lorentz force which acts against the motion of the fluid and hence causes the fluid to slow down its velocity. Fig. 3 shows that the azimuthal velocity is expected to decline with the increase in Hartmann number. This is reduced because the magnetic field creates a resistive force that decreases the rotational speed of nanofluid particles. Therefore, more suppression of the azimuthal velocity is observed in the fluid with the stronger magnetic fields. Fig. 4 temperature profile raises with the increase in the Hartmann number. An increased magnetic field creates more heat within the boundary layer as a result of the resistive (Joule heating) effects. This subsequently increases the thickness of the thermal boundary layer and increases the total temperature with Ha. Fig. 5 shows that the concentration profile decreases as the number of Hartmann number rises. Physically, the stronger the magnetic field the greater the Lorentz force that prevents diffusion of particles and species concentration in the boundary layer. Therefore, the concentration boundary layer will be thinner with an increase of Ha.

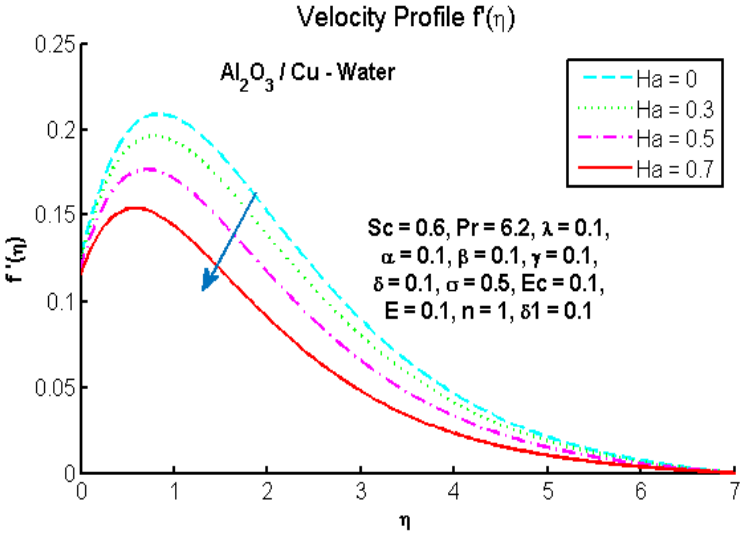

Fig. 2. Effect of Hartman number Ha on velocity profile $f'(\eta)$

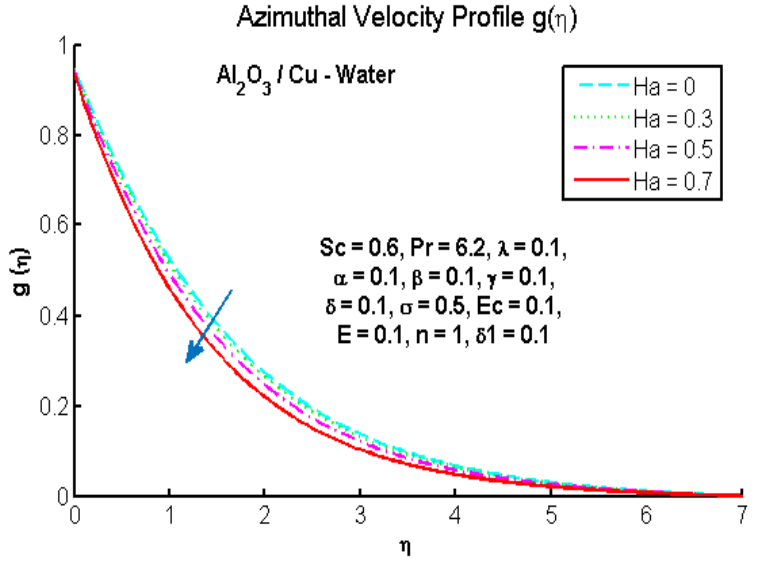

Fig. 3. Effect of Hartman number Ha on azimuthal velocity profile $g(\eta)$

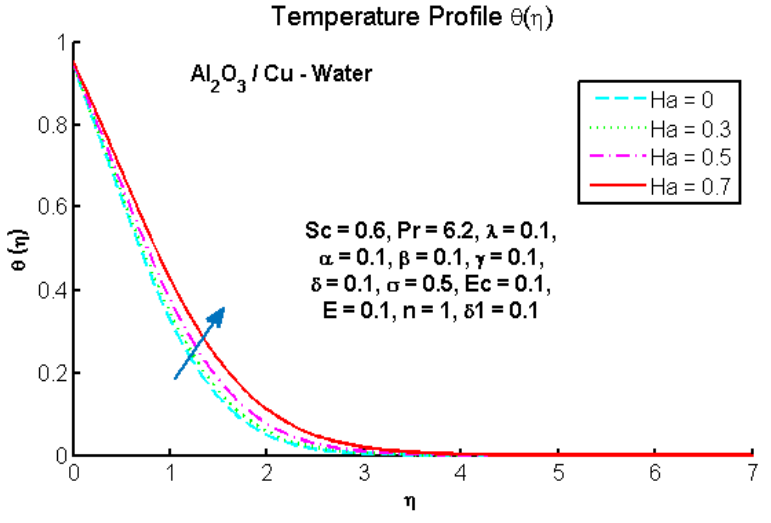

Fig. 4. Effect of Hartman number Ha on Temperature profile $\theta(\eta)$

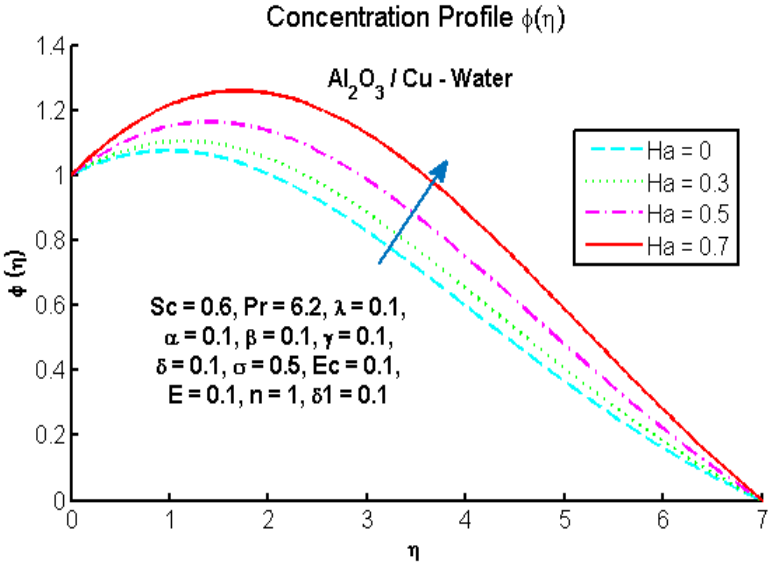

Fig. 5. Effect of Hartman number Ha on Concentration profile $\varphi(\eta)$

Fig. 6. indicates the velocity slip parameter a rises, the radial velocity f(η) decreases. This is due to the fact that when the disk surface slips, the motion being transferred to the fluid is minimized and thus the fluid moves outward at a slower rate. In Fig. 7. Shows that azimuthal velocity g(η) also decreases with a increase in α. As slip reduces the contact between the disk and the fluid, the fluid acquires less rotational motion, and therefore, this translates into weaker swirling motion. Fig. 8. indicates that, the concentration profile ϕ(η) decreases with an increase in a. Since slip occurs, the number of nanoparticles transported by the fluid reduces, and this reduces the total concentration within the boundary layer. In Fig. 9. Demonstrates that the temperature $\theta(\eta)$ decreases with an increase in thermal slip β. The heat transfer between the disk and the fluid is decreased by thermal slip and therefore the

fluid temperatures are low. Fig. 10. is used to show how the concentration slip parameter (γ) affects the concentration profile of the hybrid nanofluid. It has been noted that as γ increases, the concentration of the nanofluid in the region close to the surface reduces. Practically, the boundary slip condition decreases the direct contact between the fluid particles and the surface, which makes it weaker to transfer nanoparticles off the wall to the fluid.

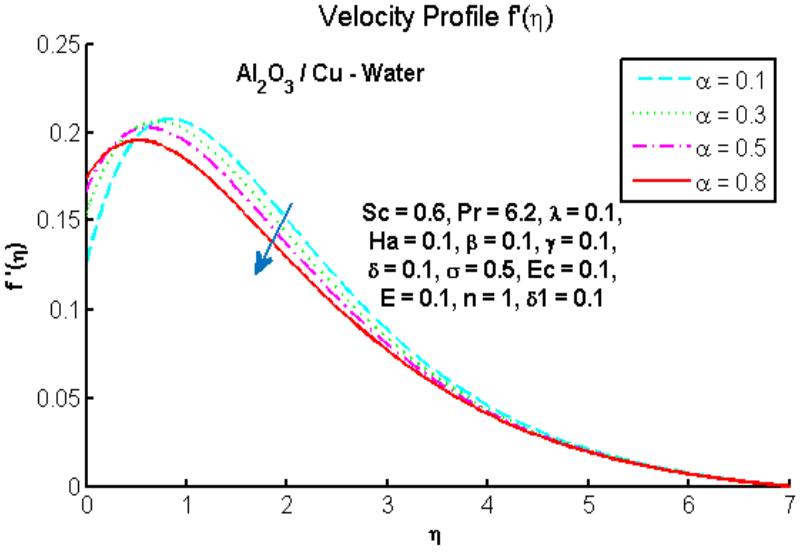

Fig. 6. Effect of velocity slip parameter α on velocity profile $f'(\eta)$

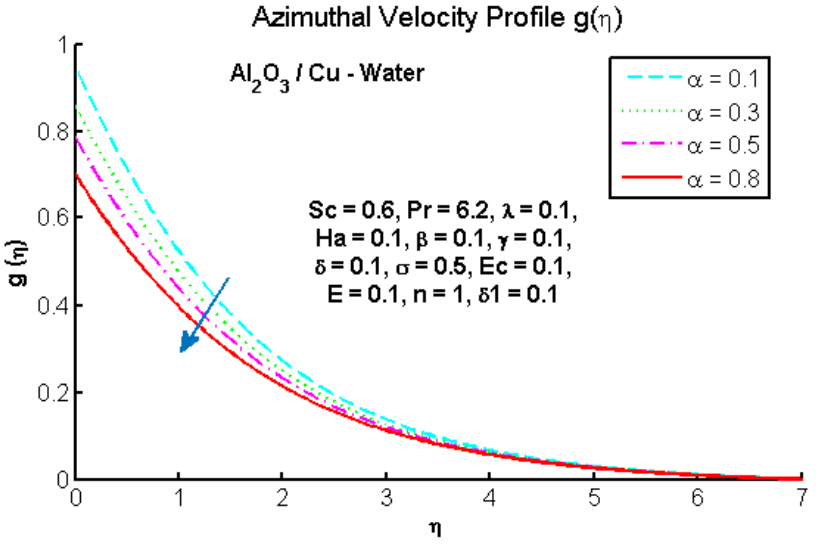

Fig. 7. Effect of velocity slip parameter α on azimuthal velocity profile $g(\eta)$

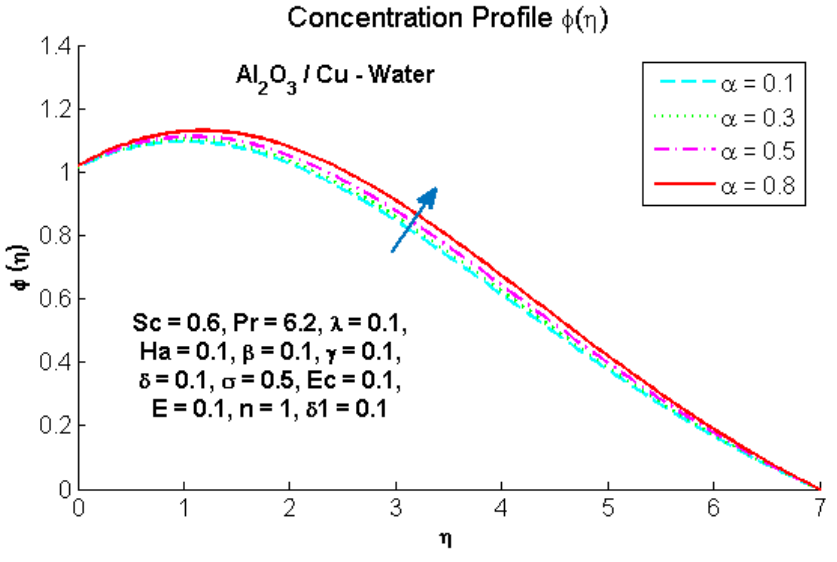

Fig. 8. Effect of velocity slip parameter α concentration profile on $\varphi(\eta)$

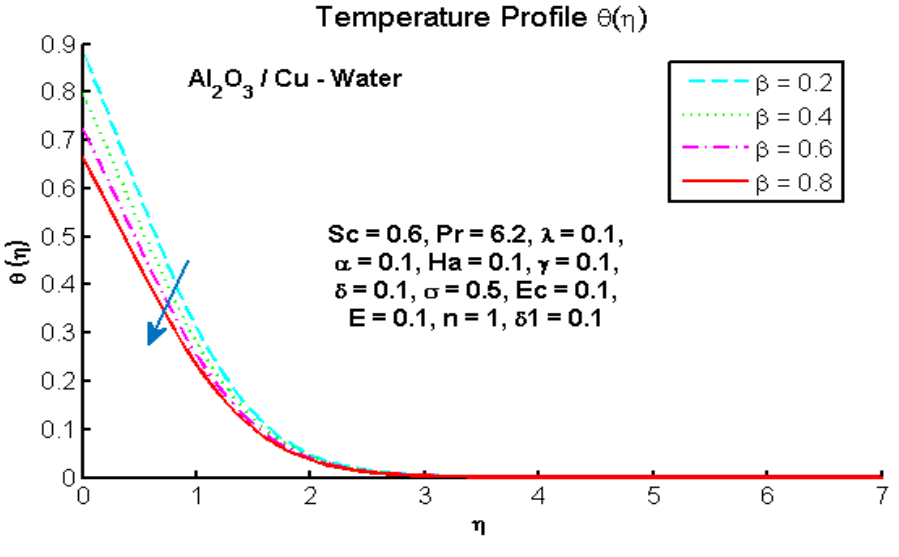

Fig. 9. Effect of thermal slip parameter β on temperature profile $\theta(\eta)$

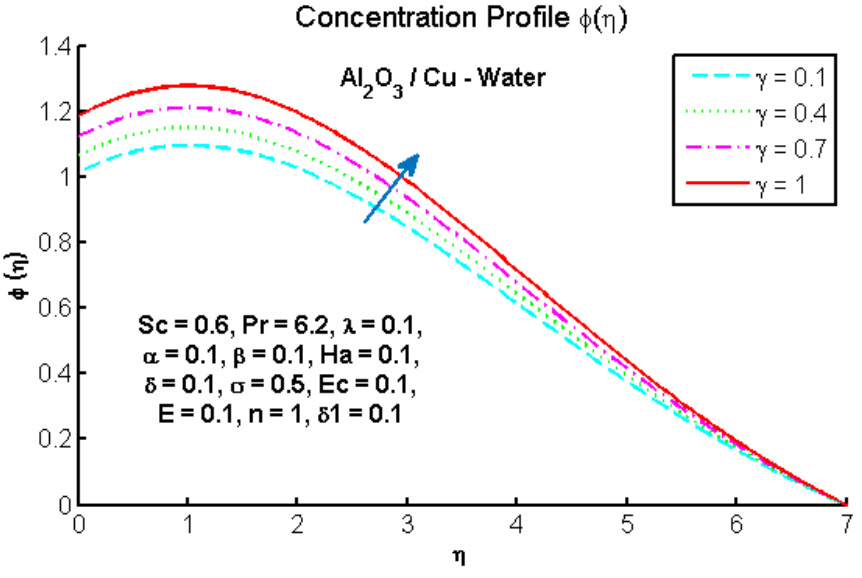

Fig. 10. Effect of concentration slip parameter γ on concentration profile $\varphi(\eta)$

Fig. 11. shows the radial velocity $f'(\eta)$ decreases as the stretching parameter (λ) increases. This is because adding more nanoparticles to the base fluid (water) increases its viscosity, making the fluid thicker and resisting its flow. The hybrid nanofluid (Cu–Al_2O_3/water) shows slower radial movement compared to pure water. Fig. 12. Shows the azimuthal velocity g(η) also decreases with higher λ. The rotating disk imparts less rotational motion to the fluid when nanoparticles are added, due to increased density and viscosity. The nanofluid swirls more slowly than the base fluid. Fig. 13. Shows the temperature θ(η) increases significantly with increasing λ. Nanoparticles have high thermal conductivity, which improves heat transfer. The highest temperature is observed at $\lambda = 0.3$, confirming that hybrid nanofluids are better for heat enhancement. In Fig. 14. Shows the concentration ϕ(η) decreases as λ increases. Higher nanoparticle concentration makes the fluid denser, which reduces the diffusion and movement of nanoparticles. The lowest concentration is seen at λ = 0.3.

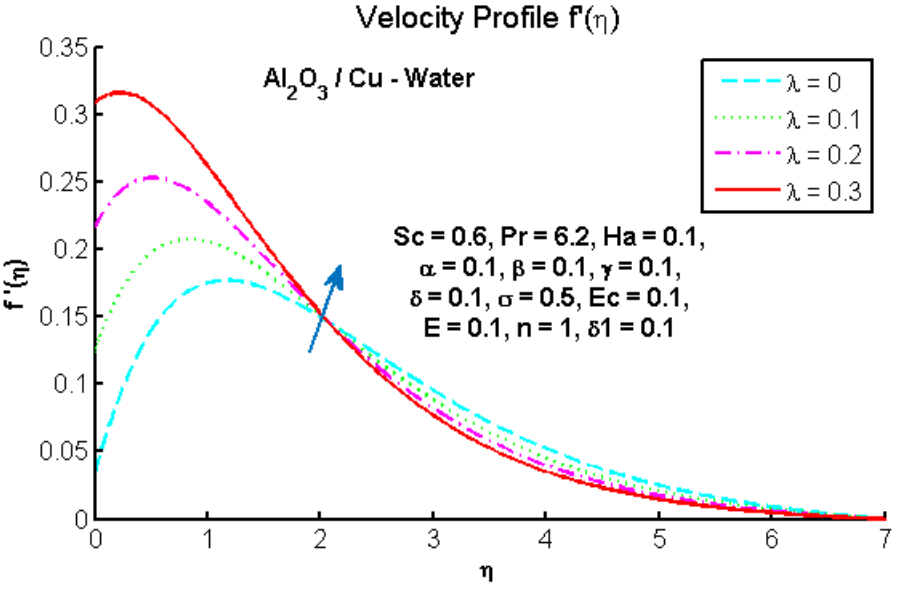

Fig. 11. Effect of stretching parameter λ on velocity profile $f'(\eta)$

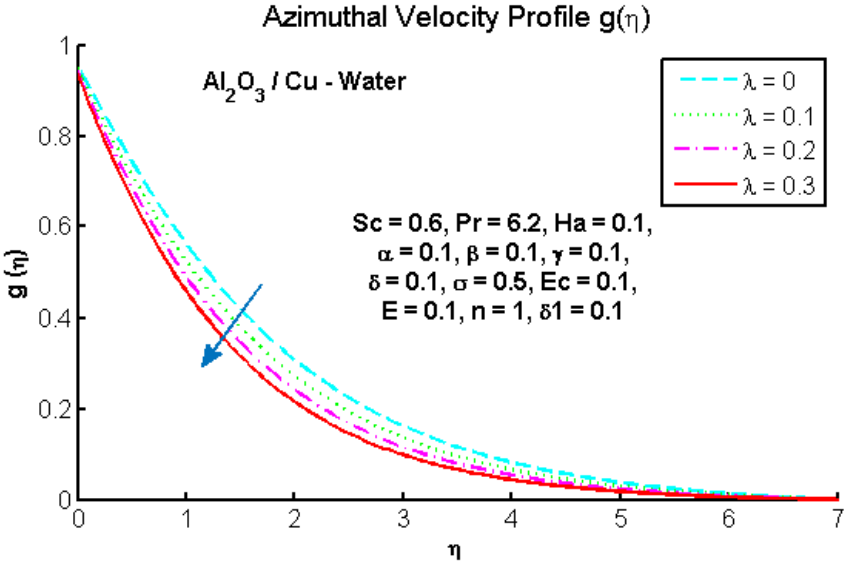

Fig. 12. Effect of stretching parameter λ on azimuthal velocity profile $g(\eta)$

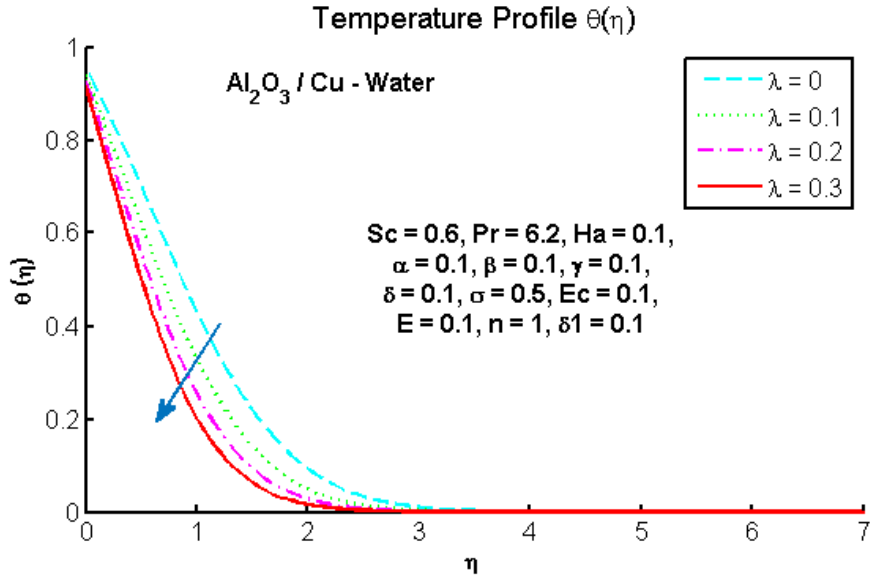

Fig. 13. Effect of stretching parameter λ on temperature profile $\theta(\eta)$

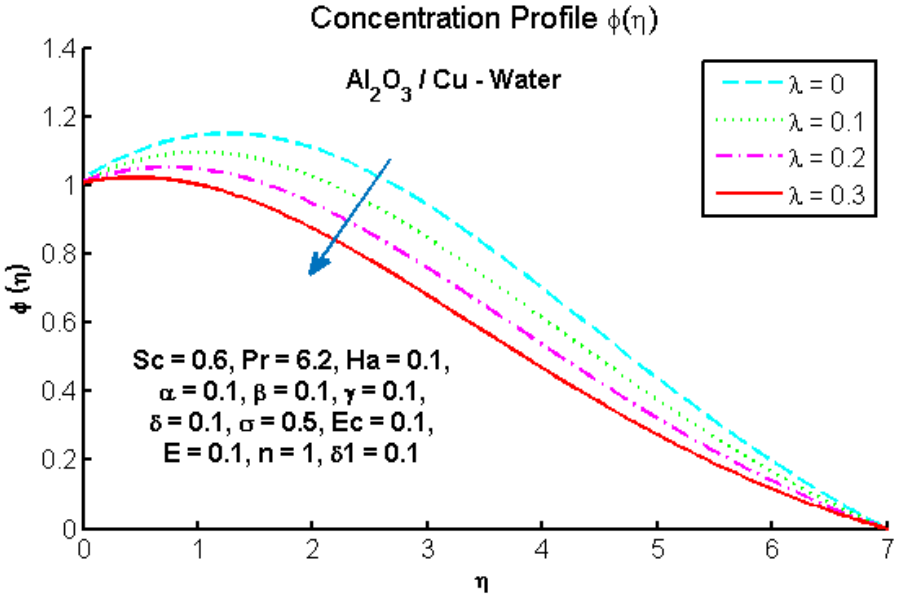

Fig. 14. Effect of stretching parameter λ on concentration profile $\varphi(\eta)$

Fig. 15. indicates that the temperature profile $\boldsymbol{\theta(\eta)}$ rises considerably with the increase of the Eckert number (Ec). Eckert number measures viscous dissipation, or, in other words, the heat produced by the friction of the fluid. Increased viscous forces cause more heat to be generated in the fluid at increased Ec causing an increase in temperature. This proves the fact that viscous dissipation is a fundamental element in augmenting thermal energy in the rotating systems. Fig. 16. illustrates the profile of concentration $\boldsymbol{\varphi(\eta)}$ declines with the increase in the Schmidt number (Sc). Schmidt number indicates the ratio between the momentum diffusivity (viscosity) and mass diffusivity. An increased Sc value

implies that the mass diffusion is slower than the momentum diffusion. Fig. 17. depicts (σ) as the parameter of the chemical reaction that is the rate at which nanoparticles are used in a chemical reaction. An increase in σ indicates an increased reaction rate.

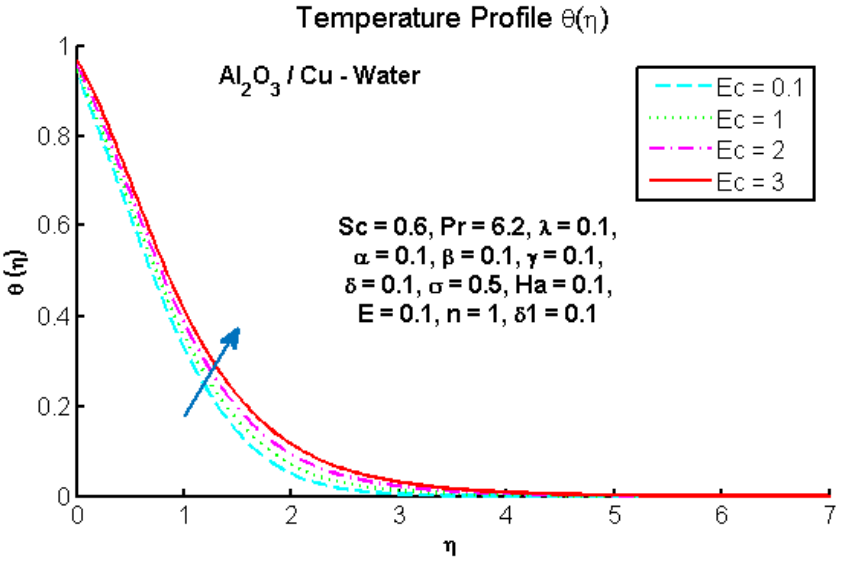

Fig. 15. Effect of Eckert number Ec on temperature profile $\theta(\eta)$

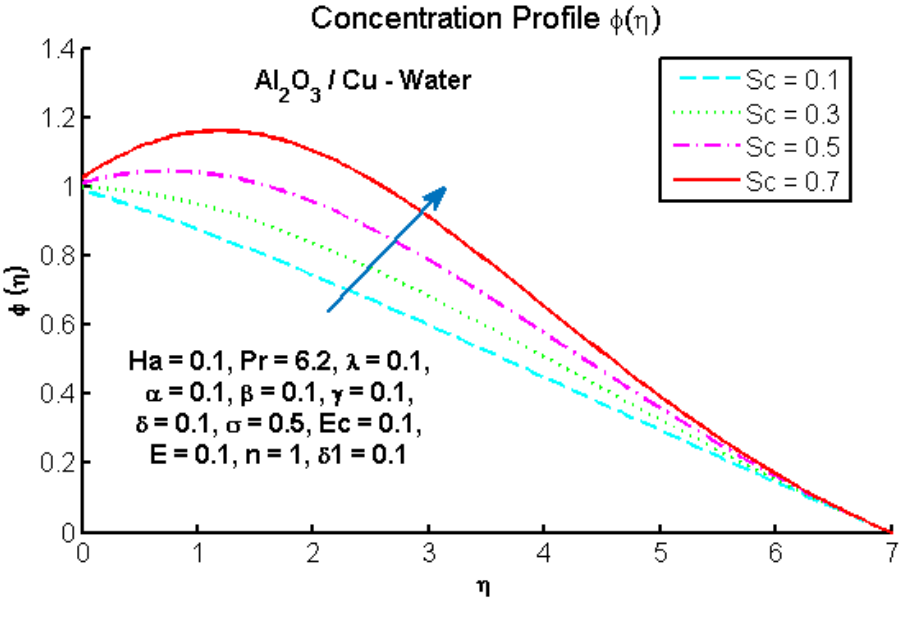

Fig. 16. Effect of Schmidt number Sc on concentration profile $\varphi(\eta)$

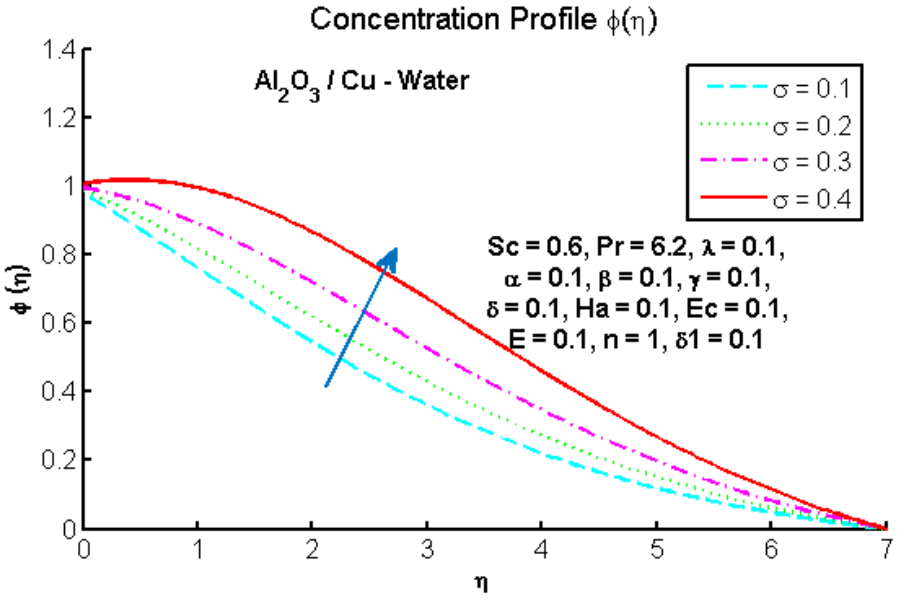

Fig. 17. Effect of reaction parameter σ on concentration profile $\varphi(\eta)$

5. Conclusion

The paper has examined the flow of a hybrid nanofluid in an exponentially stretching and rotating disk in the presence of a magnetic field. The influence of velocity slip, thermal slip, concentration slip, chemical reaction, activation energy, viscous dissipation and heat generation /absorption has been well discussed. These findings have shown that the velocity slip decreases the radial and azimuthal velocities and the thermal and concentration slips decrease the temperature and concentration profiles respectively. The Hartmann number is used to suppress the velocity components because of the Lorentz force and the parameters of activation energy and chemical reaction are greatly affecting the concentration distribution of the nanoparticles.

In addition, there is also the incorporation of copper and alumina nanoparticles that boost the effective thermal conductivity of the base fluid to increase the rate of heat transfer. It is found that the Nusselt number is always high in the case of higher ratios of thermal conductivity, which implies that hybrid nanofluids are better than conventional fluids. These results prove that hybrid nanofluids can be used in the further developments of engineering and industrial thermal management, particularly, in the fields of engineering, where effective cooling of the material and the possibility of better heat transfer are particularly important.

These findings suggest that by tuning the magnetic field and nanoparticle composition, one can optimally control both heat and mass transfer in rotating disk chemical reactors.

References

[1] S. U. S. Choi and J. A. Eastman, "Enhancing thermal conductivity of fluids with nanoparticles," in *Proc. ASME Int. Mech. Eng. Congr. Expo.*, San Francisco, CA, USA, 1995, pp. 12–17.

[2] S. Suresh, K. P. Venkitaraj, and P. Selvakumar, "Synthesis of $Cu - Al_2O_3$/water hybrid nanofluids," *Exp. Therm. Fluid Sci.*, vol. 38, pp. 54–60, 2012.

[3] M. J. Nine, H. M. Afzal, M. F. Faruque, and H. Jeong, "Hybrid nanofluids for heat transfer applications," *J. Nanopart. Res.*, vol. 16, no. 4, pp. 1–18, 2014.

[4] S. Suresh, K. P. Venkitaraj, P. Selvakumar, and M. Chandrasekar, "Effect of $Cu - Al_2O_3$/water hybrid nanofluid in heat transfer," *Exp. Therm. Fluid Sci.*, vol. 38, pp. 54–60, 2012.

[5] M. J. Nine, H. M. Afzal, and H. Jeong, "Advanced hybrid nanofluids for improved heat transfer performance," *J. Nanopart. Res.*, vol. 16, pp. 1–18, 2014.

[6] N. A. C. Sidik, M. Mahmud Jamil, W. M. A. A. Japar, and I. M. Adamu, "Graphene-based hybrid nanofluids: A review," *Int. Commun. Heat Mass Transf.*, vol. 76, pp. 16–24, 2016.

[7] T. T. Baby and S. Ramaprabhu, "Investigation of thermal properties of GO-metal hybrid nanofluids," *J. Appl. Phys.*, vol. 113, no. 12, p. 124308, 2013.

[8] M. Turkyilmazoglu, "Effects of activation energy and nonlinear thermal radiation on nanofluid flow," *Int. J. Heat Mass Transf.*, vol. 120, pp. 1161–1169, 2018.

[9] T. Von Kármán, "Über laminare und turbulente Reibung," *ZAMM - J. Appl. Math. Mech.*, vol. 1, no. 4, pp. 233–252, 1921.

[10] S. Liao and I. Pop, "Explicit analytic solution for similarity boundary layer equations," *Int. J. Heat Mass Transf.*, vol. 47, no. 1, pp. 75–85, 2004.

[11] Naseem, T., Mebarek-Oudina, F., Vaidya, H., Bibi, N., Ramesh, K. and Khan, S.U., 2025. Numerical Analysis of Entropy Generation in Joule Heated Radiative Viscous Fluid Flow over a Permeable Radially Stretching Disk. Comput Model Eng Sci, 143(1), p.1. https://doi.org/10.32604/cmes.2025.063196

[12] Naseem, T., Shahzad, A., & Mebarek-Oudina, F. (2024). Entropy Analysis in Magnetohydrodynamic Eyring-Powell GO/Blood Nanofluid over an Exponentially Stretching Sheet. International Journal of Emerging Multidisciplinary: Engineering, 2(1), 24. https://doi.org/10.54938/ijemd-engr.v2i1.11

[13] Ali, S., Shaiq, S., Shahzad, A., Sohail, M. and Naseem, T., 2024. Numerical thermal investigation of radiative magnetohydrodynamics axisymmetric Cu-Al2O3/H2O hybrid nanofluid flow over an unsteady radially stretched surface. International Journal of Ambient Energy, 45(1), p.2321210. https://doi.org/10.1080/01430750.2024.2321210.

[14] Naseem, T. and Shahzad, A., 2023. Water-based nanofluid flow and heat transfer in thin film over an unsteady stretching sheet: An entropy analysis. Numerical Heat Transfer, Part A: Applications, pp.1-25. https://doi.org/10.1080/10407782.2023.2273453.

[15] Shahzad, A., Zafar, A., Shaiq, S. and Naseem, T., 2023. Radiation effects on boundary layer flow and heat transfer of the power law fluid over a stretching cylinder with convective boundary conditions. International Journal of Emerging Multidisciplinaries: Mathematics, 2(1). https://www.ijemd.com/journal/vol2/iss1/4.

[16] Naseem, T. and Shahzad, A., 2023. Thermal transport in nanofluid across a radiated permeable sheet with irreversible effects based on the shape of the particles. International Journal of Numerical Methods for Heat & Fluid

[17] M. S. Abel, J. Tawade, and P. M. Nandeppanavar, “Heat transfer in MHD viscoelastic fluid with dissipation effects,” *Appl. Math. Model.*, vol. 36, no. 11, pp. 4848–4861, 2012.

[18] M. Turkyilmazoglu, “Exact solutions for MHD fluid flow in rotating disk boundary layer,” *Int. J. Non-Linear Mech.*, vol. 45, no. 6, pp. 623–627, 2010.

[19] L. F. Shampine, I. Gladwell, and S. Thompson, *Solving ODEs with MATLAB*. Cambridge, U.K.: Cambridge Univ. Press, 2003.

[20] Z. Said, R. Saidur, N. A. Rahim, and W.H. Azmi, “Recent advances in nanofluids,” *Renew. Sustain. Energy Rev.*, vol. 15, no. 1, pp. 164–174, 2011.

[21] M. Asma, W. A. M. Othman, T. Muhammad, F. Mallawi, and B. R. Wong, "Numerical study for magnetohydrodynamic flow of nanofluid due to a rotating disk with binary chemical reaction and Arrhenius activation energy," *Symmetry*, vol. 11, no. 10, p. 1282, Oct. 2019.

[22] M. Mustafa, A. Mushtaq, T. Hayat, and A. Alsaedi, "Rotating flow of magnetite-water nanofluid over a stretching surface inspired by non-linear thermal radiation," *PLoS One*, vol. 11, no. 2, pp. 1–16, Feb. 2016.

[23] P. Sreedevi, P. S. Reddy, and A. Chamkha, "Heat and mass transfer analysis of unsteady hybrid nanofluid flow over a stretching sheet with thermal radiation," *SN Applied Sciences*, vol. 2, no. 7, pp. 1–15, Jul. 2020.

[24] K. Hosseinzadeh, S. Roghani, A. Asadi, A. Mogharrebi, and D. D. Ganji, "Investigation of micropolar hybrid ferrofluid flow over a vertical plate by considering various base fluid and nanoparticle shape factor," *Int. J. Numer. Methods Heat Fluid Flow*, vol. 31, no. 1, pp. 402–417, 2021.

[25] K. Khanafer, K. Vafai, and M. Lightstone, “Buoyancy-driven heat transfer enhancement in a two-dimensional enclosure utilizing nanofluids,” *International Journal of Heat and Mass Transfer*, vol.

46, no. 19, pp. 3639–3653, 2003.

[26] A. Ayub, Z. Sabir, D. N. Le, and A. A. Aly, "Nanoscale heat and mass transport of magnetized 3-D chemically radiative hybrid nanofluid with orthogonal/inclined magnetic field along rotating sheet," *Case Stud. Therm. Eng.*, vol. 26, pp. 101193, 2021.

[27] R. I. Yahaya, N. M. Arifin, I. Pop, F. M. Ali, and S. S. P. M. Isai, "Flow and heat transfer analysis of hybrid nanofluid over a rotating disk with a uniform shrinking rate in the radial direction: Dual solutions," *Sindh Journal of Innovations and New Technologies (SIJIN)*, vol. 1, no. 1, pp. 29–44, Jun. 2024.

[28] M. Turkyilmazoglu, "Nanofluid flow and heat transfer due to a rotating disk," *Computers & Fluids*, vol. 94, pp. 139–146, May 2014.

[29] A. Abd-Elmonem et al., "Case study of heat generation/absorption and activation energy on MHD hybrid nanofluid (GO-MoS_2/water) flow owing to a rotating disk," *Case Studies in Thermal Engineering*, vol. 51, pp. 103632, 2023.